# S235JR steel corrosion behavior in neutral chloride media

Khaoula Nasr[a*], Michele Fedel[b], Flavio Deflorian[b], Nizar Bellakhal[c], Nébil Souissi[a]

[a] *University of Tunis El Manar, Institut Préparatoire aux Etudes d'Ingénieurs d'El Manar, BP 244 El Manar II, 2092 el Manar, Tunisia.*
[b] *University of Trento, Department of industrial engineering, Via Mesiano 77, 38123 Trento, Italy.*
[c] *University of Carthage, Institut National des Sciences Appliquées et Technologie, 1080 Tunis Cedex, Tunisia.*

(Received: 24 May 2016, accepted: 02 July 2016)

**Abstract:** We investigated the electrochemical behavior of S235JR steel in chloride media. The results of studying the effect of chloride concentration were reported and compared to those obtained for ordinary carbon steel (OS). Potentiodynamic polarization and cyclic voltammetry techniques were employed. For S235JR steel, it was revealed that the corrosion rate increased at higher chloride concentration and a first order kinetics was obtained. The pitting potential varied linearly with the logarithm of chloride concentration and the slope value was 110.9 mV/decade. In comparison with the ordinary carbon steel corrosion behavior, S235JR steel showed generally a better general corrosion resistance in chloride media. This was reflected by a lower value of corrosion current density equal to 8.6 mA $cm^{-2}$ compared to OS (28.3 mA $cm^{-2}$). The pitting potential determined for S235JR steel (-336 mV/SCE) was more positive than the one of OS (-365 mV/SCE) highlighting that S235JR steel is less subjected to pitting corrosion.

**Keywords:** S235JR steel, chloride, pitting, polarization, voltammetry.

## INTRODUCTION

With the rapid development of petroleum industry, tanks play an increasing role in oil and derivatives storage. These tanks are exploited in an open park which is mostly situated in a marine environment. Thus, materials surfaces are subjected to severe corrosion. To prevent environmental disasters and minimize activities disruption, it is important to find reliable methods for materials preservation. This is possible only when understanding the corrosion mechanism evolved.

Hydrocarbon storage tanks are made of carbon steel due to its excellent mechanical properties and its low cost. Several investigations have been concerned on discovering its corrosion mechanism in neutral media containing chloride ions [1]. Although S235JR carbon steel is used as a building material for hydrocarbon storage tanks, there is a lack of studies dealing with its corrosion phenomenon in chloride media. In fact, Trzaska and al. [2] compared the electrochemical behavior of pure iron and S235JR steel in NaCl 0.5M solution employing potentiodynamic and impedance spectroscopy techniques. The authors reported a lower corrosion resistance of S235JR steel due to alloying elements addition and material heterogeneity. Popescu *and al*. [3] also aimed to study the corrosion of S235JR steel and austenitic 304 stainless steel in both HCl 0.5 M and NaCl 3% media by potentiodynamic technique. The results confirmed that regardless of the corrosive solution, S235JR steel corrosion rate was higher. In the other hand, hydrochloric acid medium was much more aggressive to S235JR steel than sodium chloride solution.

The purpose of this paper is to extend our knowledge on S235JR steel corrosion in neutral aerated chloride media. The effect of chloride anions concentration on cyclic voltammetry and polarization investigations responses was evaluated.

## EXPERIMENTAL

The specimens under investigation were S235JR steel and ordinary carbon steel (OS)

* Corresponding author, e-mail address : nasr.khawla@gmail.com

cylinders provided by the Tunisian Refinery Industries Company and the Tunisian Iron and Steel Company, respectively. Their exposed area was 0.196 $cm^2$. Before immersion in the electrolyte, the electrodes surfaces were hand-polished with emery papers up to the grade of 1200, rinsed in deionized water and then air-dried.

The corrosive media was neutral aerated sodium chloride solutions prepared from ultrapure reagents.

A classical three-electrode cell assembled with a saturated calomel electrode (SCE) as reference and a separate Pt-wire electrode with a bottom diameter of 12 mm as auxiliary electrode was used for the electrochemical study.

Electrochemical experiments were conducted on an Autolab 302N Potentiostat. Nova 1.10 software was used for instrumentation control and data treatments. Before carrying any experiment, we determined the considered steel open circuit potential (OCP) value after exposition to the corrosive media for 5 minutes. After, anodic and cathodic curves were obtained separately. The anodic branch was recorded by changing linearly the electrode potential from the previously noted OCP value toward more positive values until the end of the experiment at -0.2 V/SCE. In order to record the cathodic branch, we did another experiment by varying the potential from the OCP value to -1.5 V/SCE. Considering the cyclic voltammetry curves, we swept the potential from the determined OCP value toward higher potential values until the current value reached 2 mA. At this moment, the potential reversed back and varied linearly until -1.5 V/SCE.

**Table I**. Investigated steels chemical composition.

| Steel | Mn (w%) | Cu (w%) | Si (w%) | Cr (w%) |
|---|---|---|---|---|
| **S235JR** | 1.05 | - | - | - |
| **Ordinary Steel** | 0.91 | 0.29 | 0.27 | 0.15 |

Optical images were done using an optical microscope Nikon SMZ25. A Phillips XL30 SEM-EDS with an energy dispersive detector was employed to record the EDS spectra of the tested samples.

## RESULTS AND DISCUSSION

### 1. Materials characterization

The chemical composition of S235JR steel and OS was determined by EDS. Figure 1 illustrated the obtained spectra and Table I gathered the elements weight percentages. Mn was revealed as the major alloying element for both materials.

The microstructure of the steels was revealed using Nital 2% as etching reagent [4]. The specimens were polished until the surface was like a mirror and then etched during 10 s. Figure 2 showed the obtained images. A difference in the microstructure of the steels was detected. For S235JR steel, two dominant phases, banded ferrite (clear parts) and pearlite (dark regions) were observed [5,6]. Pearlite was a mixture of lamellar ferrite (alpha-iron) and cementite. OS microstructure was characterized by the presence

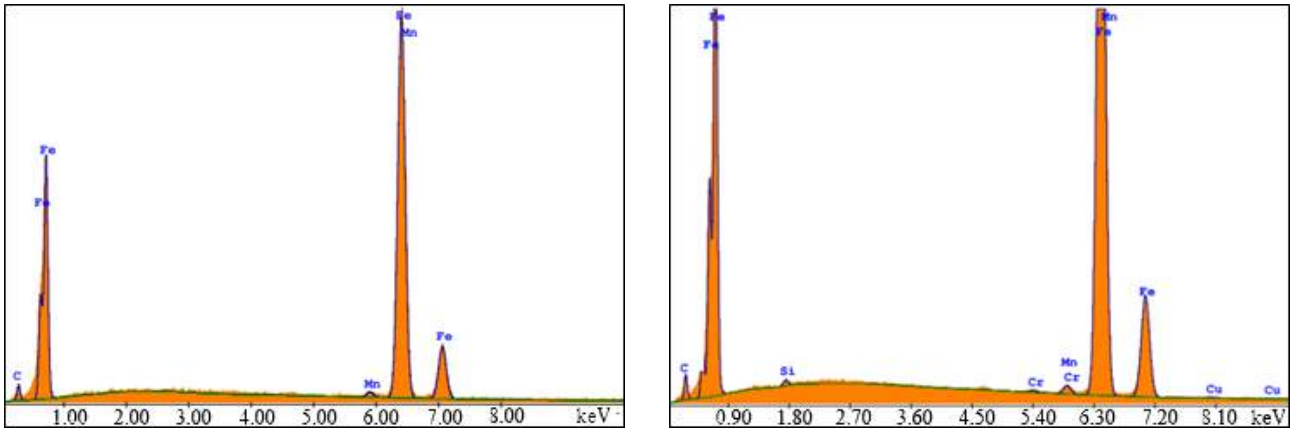


**Figure 1**. EDS spectrum of bare (a) S235JR steel (b) Ordinary steel.

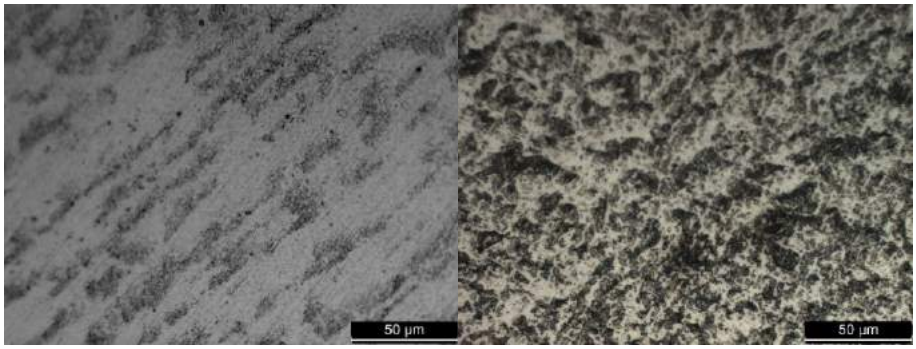


**Figure 2**. Metallographic images of (a) S235JR steel (b) OS.

of granular bainite added to ferrite and an important amount of pearlite [4].

## 2. S235JR and ordinary carbon steels corrosion resistance in chloride media

The anodic and cathodic polarization curves of S235JR steel and OS were plotted in NaCl 0.5 M after an immersion time of five minutes at 1 $mVs^{-1}$ scan rate at 25°C. The curves obtained were gathered in Figure 3.

Independently on the material, four distinct domains could be distinguished. In fact, for voltages up to -1V/SCE, a rise in current value was noticed. This was due to the reduction of $H_2O$.

The second potential domain was between -1 V/ SCE and $E_1$($E_1$ = -0.6 V/SCE) where a current plateau was observed. It corresponded to the limit diffusion current ($J_L$) resulting from dissolved oxygen reduction. As shown on Figure 3, $J_L$ was 38 µA $cm^{-2}$and 118 µA $cm^{-2}$ for S235JR steel and OS, respectively.

The curves with linear scale were characterized by a particular potential below which there was a sudden increase in current denoting the initiation and propagation of pitting corrosion. This critical potential was called the pitting potential Epit [7,8]. A region of mixed charge transfer and mass transport kinetics was situated in the range [$E_1$,Epit] and it was attributed to Tafel domain.

The fourth area was located in the potential interval corresponding to voltages greater than Epit. It was attributed to pitting corrosion domain.

In the neighborhood of the Tafel region, the extrapolation of the anodic and cathodic Tafel lines back to the corrosion potential Ecor allowed determining anodic Tafel slope βa, cathodic Tafel slope βc and corrosion current density Jcor.Then, the proportionality constant B and the polarization resistance R were calculated through the following equations [9]:

$$B = \beta a * \beta c / 2.3 * (\beta a - \beta c) \quad (1)$$

$$Rp = B / Jcor \quad (2)$$

We compared the main determined corrosion parameters of both steels in NaCl 0.5M solution with those of other steels reported in literature. Results were summarized in Table II.

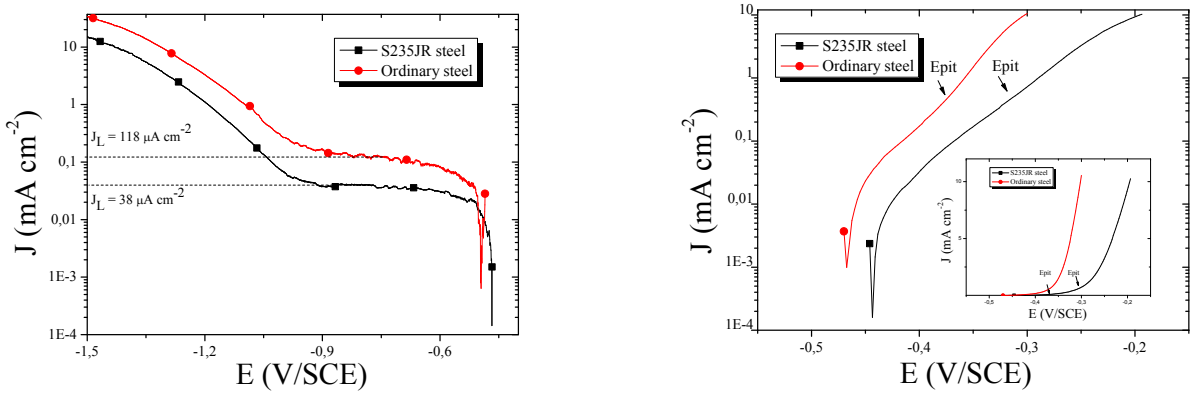


**Figure 3**. Cathodic (a) and anodic (b) polarization curves obtained on S235JR steel and OS in aerated NaCl 0.5M.

**Table II**. Review of Tafel parameters for steel in chloride media.

| Medium | material | Scan rate (mv $s^{-1}$) | Immersion time (min) | Ecor (mV/SCE) | βa ($mV^{-1}$) | -βc ($mV^{-1}$) | Jcor (μA $cm^{-2}$) | B ($mV^{-1}$) | Rp (Ω $cm^2$) | Ref |
|---|---|---|---|---|---|---|---|---|---|---|
| **0.5M NaCl** | S235JR (Mn) | 1 | 5 | -456 | 82 | 100 | 8.6 | 20 | 2278 | Our work |
| **0.5M NaCl** | OS (Mn,Cu,Si,Cr) | 1 | 5 | -476 | 60 | 73 | 28.3 | 14 | 506 | Our work |
| **0.5M NaCl** | S235JR (Cu, Ni,Cr,Si,Mn) | 0.3 | - | -641 | - | - | 93 | - | - | [2] |
| **3% NaCl** | S235JR (Mn) | 1 | - | -608 | 86 | 399 | 44.21 | 30.76 | 696 | [3] |
| **3.5% NaCl** | 1018 carbon steel | 1 | 30 | -542 | 391 | 355 | 12.23 | 81 | 6620 | [11] |
| **3.5% NaCl** | Mild Steel | 0.1 | 60 | -1007 | 69 | 109 | 92.15 | 18.37 | 199 | [12] |

For S235JR steel, Ecor value was -456 mV/ SCE. This value was a little bit nobler compared with that measured for OS. It was noticed that the values reported for S235JR steel [2,3] were more negative than the one delivered by our study. Such divergence could be due to the different scan rate adopted or the surface finish [10]. In fact, a variation in the scan rate could induce the shift of the corrosion potential and different surface preparations before the experiment, generated an increase or decrease in the corrosion potential value [10]. In the other hand, Ecor value exhibited by our work for S235JR was quite similar to that obtained in Mahmoud and al. study [11]. In fact, a little difference was observed in spite of the distinct exposition time and chloride concentration used. It should be noted that Khaled study [12] delivered a very negative value of Ecor (-1000 mV/SCE) which could be due to the low scan rate and the long exposure time adopted.

The apparent anodic Tafel slope βa was found to be close to 82 $mV^{-1}$ for S235JR steel. This value was higher than the one observed for OS (60 $mV^{-1}$), highlighting a little change in the mechanism of metal dissolution. We remarked that our βa value delivered for S235JR was quite similar to that reported in Khaled study [12]. This value of 82 $mV^{-1}$ was in accordance with the published values ranging from 30 $mV^{-1}$ to 120 $mV^{-1}$ for many materials in different environments [13]. Contrarily, Mahmoud and al. study [11] showed almost three orders of magnitude higher values.

We measured an apparent cathodic Tafel slope βc of 100 $mV^{-1}$for S235JR steel. The different value (70 $mV^{-1}$) observed for OS indicated a change in the oxygen reduction process evolved [14]. The value of βc that we reported was consistent with the generally published value of about 120 $mV^{-1}$for the cathodic reactions of oxygen reduction in alkaline solutions [15]. Near value of βc equal to 109 $mV^{-1}$was delivered by Khaled and al. study [12]. In the other hand, two investigations [3,11] reported much higher values of βc around 300 $mV^{-1}$.

For the corrosion current density Jcor, S235JR steel exhibited a low value of 8.6 μA $cm^{-2}$ whereas a higher value equal to 28.3 μA $cm^{-2}$ was estimated for OS. Such result indicated that S235JR steel uniform corrosion rate was lower than OS one. The notably higher values of Jcor reported [2,3,12] suggested that our adopted experimental conditions for S235JR steel provided better protection against corrosion. Only Mahmoud and al. [11] investigation delivered a value quite similar to that obtained in our study for S235JR steel.

The proportionality constant B values calculated for both steels were quite similar i.e. 20 $mV^{-1}$ and 14 $mV^{-1}$ for S235JR steel and OS respectively. For the same media, we observed a wide range of values varying from 14 to 81 $mV^{-1}$. This deviation could be attributed to different experimental conditions and to varying states of the surface condition [16].

Concerning the linear polarization resistance Rp, S235JR steel delivered a value of 2278 Ω $cm^2$ which was higher than the one obtained for OS. Based on the assumption that polarization resistance was inversely proportional to the

corrosion current density [17], we could conclude that S235JR steel corroded slower than OS. The various values of Rp reported for steel in chloride media reflected different tendency for uniform corrosion depending on the experimental conditions.

It was worth noting that the considered investigations for the comparison obtained the polarization curves by changing the potential from cathodic values to greater values. Contrarily, we obtained separately the anodic and cathodic polarization curves starting from the OCP. This could be the main reason for the observed different values.

In order to scrutinize the corrosion behavior of the studied steels, we used cyclic voltammetry. Figure 4 showed the cyclic voltammograms obtained for both steels after immersion for 5 minutes in NaCl 0.5 M at a scan rate of 1 mV $s^{-1}$.

Both curves examination indicated the presence of the critical potential Epit followed by a current sudden increase. When the potential scan was reversed back, we observed an hysteresis loop denoting the pitting attack occurring [18]. After that, there was a rapid decrease of current until it equal zero at a special potential. This potential was characterized by the repassivation of the formed pits and was hence called repassivation potential (Erep) [18,19]. At more cathodic potentials, a current plateau was detected reflecting the dissolved oxygen reduction. Reaching potentials higher than -1 V/SCE allowed the occurring of water reduction. The Epit and Erep values were extracted and recapitulated in Table III.

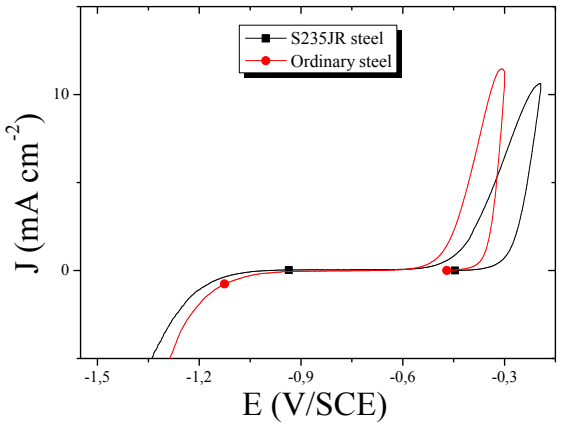


**Figure 4**. Cyclic voltammograms for S235JR steel and OS in NaCl 0.5M.

**Table III**. Values of Epit and Erep for both steels in NaCl 0.5M.

| Steel | Epit (mV/SCE) | Erep (mV/SCE) |
|---|---|---|
| **S235JR** | -336 | -978 |
| **OS** | -365 | -667 |

For S235JR steel, Epit value was around -300 mV/SEC. This value was in accordance with the recently published values for steel in aerated chloride media [20]. It was noticed that Epit value of S235JR steel was higher than the one of OS. It was reported that nobler Epit values indicated a less tendency to pitting corrosion [19,21]. Hence, one can say that S235JR steel was less subjected to pitting corrosion than OS. We could remark that Erep value was more negative for S235JR steel suggesting that it needed more time to repassivate.

## 3. Influence of chloride concentration

In order to evaluate an eventual effect of chloride anions concentration on the electro-chemical behavior of S235JR steel, we recorded the polarization curves for S235JR steel and OS after five minutes exposure to different chloride concentrations, ranging between 0.25 M and 1 M at a scan rate of 1 $mVs^{-1}$. The obtained curves were illustrated in Figure 5.

Independently on the material, it was noticed that when the halide content increased, the anodic current density increased since more chloride anions are available on the steel surface. The cathodic current density decreased slightly with increasing chloride concentration. Such a result might be due to the higher solution viscosity obtained with chloride concentration increase [22]. Table IV recapitulated the corrosion parameters obtained for the investigated steels.

For both steels, Ecor shifted towards active values with increasing amounts of halide anions corresponding to a more aggressive media.

The anodic and cathodic Tafel slopes did not show a noticeable change with the increasing aggressive ions content suggesting that the metal dissolution and oxygen reduction mechanisms were not influenced by the chloride anions concentration.

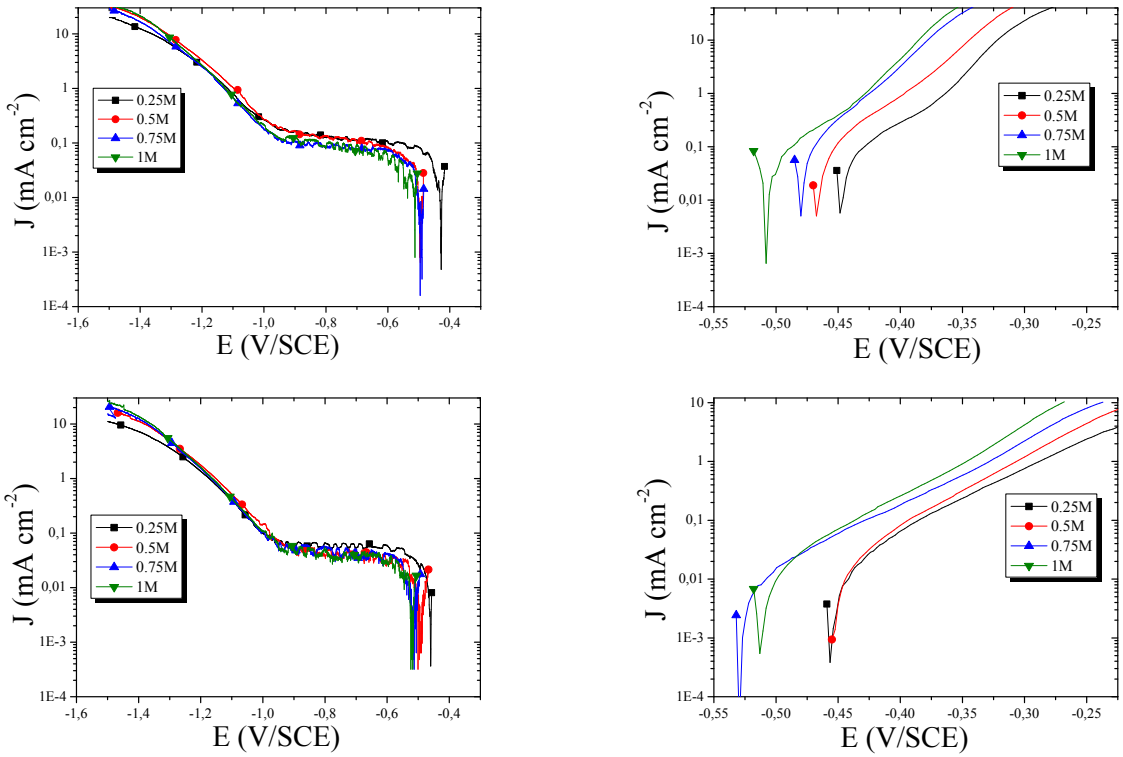


**Figure 5**. Cathodic polarization curves (a) for OS and (c) for S235JR steel and anodic polarization curves (b) for OS and (d) for S235JR steel with different concentrations of chloride anions.

Independently on the material, Jcor values increased when chloride concentration rised. In fact, the enhancing effect of NaCl concentration on the anodic process predominated its drop influence on the cathodic current density, which generated a marked increase of Jcor [22].

Varying the chloride content did not influence the constant proportionality value B which value remained almost the same for each steel. This was expected since B characterized a material in a definite environment.

For the polarization resistance Rp, it was remarked that increasing the amount of halide anions lowered its value for both steels, indicating the enhancement of the uniform corrosion in more aggressive media.

**Table IV**. Electrochemical indicators for S235JR and OS in different chloride concentrations.

| [$Cl^-$] (mol $L^{-1}$) | Steel | Ecor (mV/SCE) | βa ($mV^{-1}$) | -βc ($mV^{-1}$) | Jcor (μA $cm^{-2}$) | B ($mV^{-1}$) | Rp (Ω $cm^2$) |
|---|---|---|---|---|---|---|---|
| **0.25** | **S235JR** | -445 | 79 | 75 | 6.3 | 16.7 | 2655.2 |
| | **OS** | -468 | 52 | 59 | 15.1 | 12.0 | 795.8 |
| **0.5** | **S235JR** | -456 | 82 | 100 | 8.6 | 19.6 | 2277.8 |
| | **OS** | -476 | 60 | 73 | 28.3 | 14.3 | 506.0 |
| **0.75** | **S235JR** | -510 | 84 | 88 | 18.3 | 18.7 | 1021.1 |
| | **OS** | -480 | 61 | 75 | 35.4 | 14.6 | 413.2 |
| **1** | **S235JR** | -514 | 81 | 64 | 22 | 15.5 | 706.6 |
| | **OS** | -491 | 62 | 68 | 41.1 | 14.1 | 343.1 |

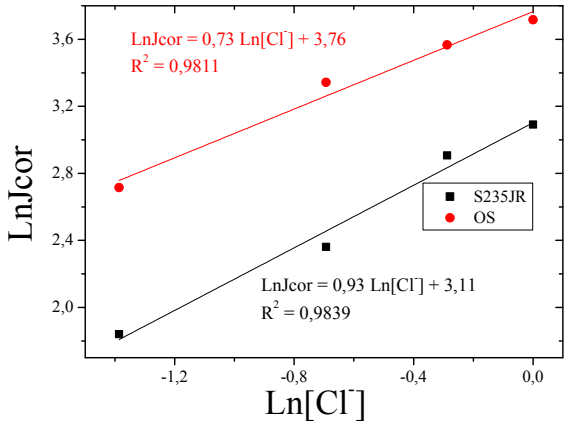


**Figure 6**. Plot of LnJcor against Ln[$Cl^-$] for both steels.

Based on the results below, the relation between the steels corrosion rate and chloride concentration could be expressed using the following kinetic rate equation [23]:

$$logJcor = log\ (F\tau k_2[Cl^-]^n \left(\frac{k_1}{k_{-1}}\right)/ (1 + k_{-2}\tau/m_{FeCl^-}) + EF/2.3RT) \quad (3)$$

Where Jcor was the corrosion current density, τ was the total surface site concentration, $m_{FeCl^-}$ was the ratio between the $FeCl^-$ diffusion coefficient and the diffusion thickness layer, F was the Faraday constant, E was the electrode potential and $k_2$ and $k_{-2}$ were the desorption and adsorption rate constants. $k_1$ and $k_{-1}$ were expressed as follows [23]:

$$k_1(t) = k_a \exp\left(\frac{\alpha_a FE}{RT}\right) \quad (4)$$

$$k_{-1}(t) = k_c \exp\left(\frac{-\alpha_c FE}{RT}\right) \quad (5)$$

The chloride order of reaction could be expressed by the equation (6) [23] and the slope of the linear dependence of LnJcor on Ln[$Cl^-$] gave the corresponded value.

$$n_{Cl^-} = \left(\frac{\delta LnJcor}{\delta\ Ln[Cl^-]}\right)_{\tau,E} \quad (6)$$

Figure 6 illustrated the linear relationship between LnJcor and Ln[$Cl^-$] for both steels.

We estimated a reaction order values of 0.93 and 0.73 for S235JR steel and OS respectively, with good correlation coefficient values up to 0.98. The obtained value of n was around unity for S235JR steel, which indicated a first order kinetics for this steel with respect to chloride concentration in neutral aerated sodium chloride medium. The value of 0.73 which was far from 1 delivered for OS reflected a different reaction kinetic. For the corrosion of stainless steel (Fe6956) in HCl solution, Oguike and al. [24] reported 0.78 as n value that was close to the calculated for OS.

Figure 7 represented the cyclic voltammograms recorded for both steels with the chosen range of chloride concentrations.

Independently on the material, it was remarked that higher amounts of chloride anions induced the displacement of the hysteresis on the active direction and its size growth. This observation indicated the enhancement of pitting attack with chloride concentration increase. Epit and Erep values were recapitulated in Table V.

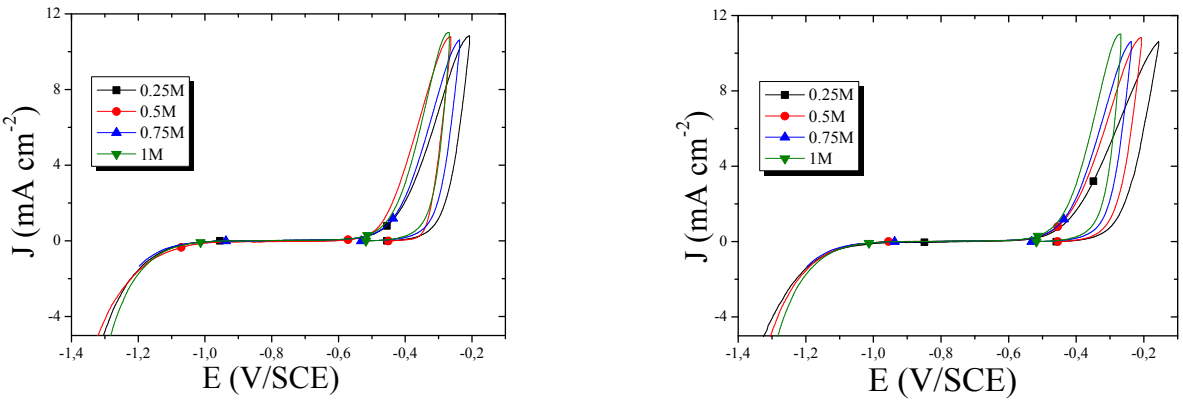


**Figure 7**. Cyclic voltammograms for different concentrations of chloride anions for (a) OS (b) S235JR steel.

**Table V**. Epit and Erep values for S235JR and OS in different chloride concentrations.

| Chloride concentration (mol $L^{-1}$) | Steel | Epit (mV/SCE) | Erep (mV/SCE) |
|---|---|---|---|
| **0.25** | **S235JR** | -307 | -706 |
| | **OS** | -336 | -608 |
| **0.5** | **S235JR** | -336 | -978 |
| | **OS** | -365 | -667 |
| **0.75** | **S235JR** | -360 | -592 |
| | **OS** | -392 | -810 |
| **1** | **S235JR** | -373 | -1035 |
| | **OS** | -403 | -996 |

For both steels, with increasing chloride concentration, Epit shifted towards negative values suggesting the decrease of the pitting resistance. Concerning Erep, we remarked that independently on the steel its values become more negative with increasing halide content, which was the result of the pitting enhancement.

In order to understand the influence of chloride concentration on the pitting potential, we plotted Epit as function of pCl (pCl =-log[$Cl^-$]) for both steels. Figure 8 represented the obtained curves.

For both steels, there was a linear dependence of Epit on pCl that was reported for different materials in contact with an aggressive solution [19,20]. This linear relation could be represented by the following equation:

$$Epit = \alpha + \beta\, pCl \qquad (7)$$

with α and β were constants and Epit (mV).

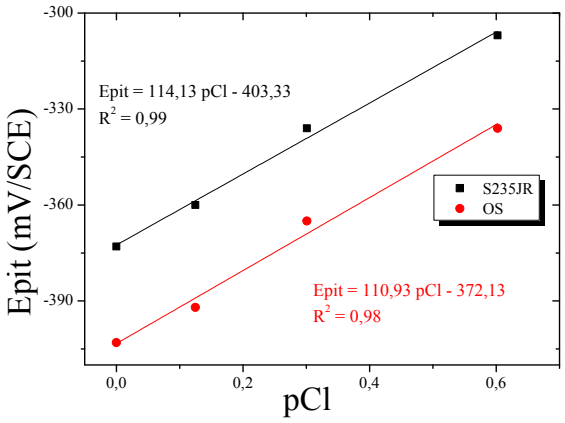


**Figure 8**. Plot of Epit against pCl for both steels.

For S235JR steel, we found that α was -403.33 mV whereas for OS it equaled to -372.13 mV. It was noticed a little difference Δα of -31.2 mV ($\Delta\alpha = \alpha_{S235JR} - \alpha_{OS}$). Hassan and al. [19] reported α value of -409 mV for a mild steel in a chloride citrate solution, which was quite similar to that obtained for S235JR steel.

β value equaled to 110.9 mV/decade for S235JR steel and OS showed a value of 114.13 mV/decade. It was reported that β value characterized the susceptibility of the passive layer to pitting [19]. Since a little difference Δβ ($\Delta\beta = \beta_{S235JR} - \beta_{OS}$) of 3.23 mV/decade was obtained, we could say that S235JR steel and OS have near pitting resistance in chloride media. The calculated values for S235JR steel and OS were quite similar to that found by Hosni and al. [20] (114 mV/ decade) for AISI 316L steel in aerated chloride solution at 25°C.

## 4. Explanation of the different steels corrosion behaviors

The observed difference on the electro-chemical behavior of S235JR steel and OS could be explained in terms of electrochemical composition and microstructure.

Exploring the literature, Jang and al. [25] reported that increasing amounts of copper (0.2% and 0.35%) improved the uniform corrosion resistance and inversely promoted the pitting attack of steel in chloride solution. Concerning Cr addition, Park and al. [26] investigated the effect of Cr (0 and 0.5%) on the corrosion resistance of low-alloy steels containing Cu in a concentrated sulphuric acid solution with HCl. They concluded

that the presence of Cr increased both the uniform and pitting corrosion of the steel since copper presence enhanced the Cr segregation at the grain boundaries.

OS contained Cr and Cu as alloying elements whereas S235JR did not. Based on the review below, this could explain the higher tendency of OS for uniform and pitting corrosion. Added to that, OS contained more alloying elements than S235JR steel. This might introduce an heterogeneity to OS surface promoting its corrosion process.

It was well reported that the carbon steels corrosion performance was influenced by their microstructure [5,6]. For this reason, the difference observed on the microstructure of S235JR steel and OS could contribute to the better corrosion resistance of S235JR steel.

## CONCLUSION

The electrochemical behavior of S235JR steel in 0.5 M neutral aerated chloride media was investigated and compared to that exhibited by an ordinary carbon steel (OS).

It was observed that chloride concentration had an effect on the corrosion behavior of S235JR steel reflected by a first order kinetic. Potentiodynamic measurements indicated that the corrosion rate increased with chloride contents and pitting potential decreased linearly with the logarithm of halide concentration.

When compared to OS, S235JR steel was less subjected to uniform and pitting corrosion. Such result could be explained by the observed difference in the steels microstructure.

## REFERENCES


[1] M.A. Deyab, S.T. Keera, *Egyptian Journal of Petroleum*, **2012**, *21*, 31-36.

[2] M. Trzaska, *Corrosion Resistance*, Dr Shih (Ed.), **2012**, *18*, 398-420.

[3] M. Popescu, E. Simona Cutean, R.Alexandru Rosu, M. Bobina, Brno, *Czech Republic,* **2012**, *5*, 23-25.

[4] S. Qu, Xiaolu Pang, Y. Wang, K. Gao, *Corrosion Science*, **2013**, *75*, 67-77.

[5] D. Cloverly, B. Kinsella, B. Pejcic, R. De Marco, *Journal of Applied Electrochemistry*, **2005**, *35*, 139-149.

[6] S.I. Al-Rubaiey, E.A. Anoon, M.M. Hanoon, *Eng. &Tech. Journal*, **2013**, *31*, 1825-1836.

[7] E.M. Sherif, *Int. J. Electrochem. Sci.*, **2011**, *6*, 3077-3092.

[8] L. Cáceres, T. Vargas, L. Herrera, *Corrosion Science*, **2009**, *51*, 971-978.

[9] M. Stern, R.M. Roth, *Journal of Electrochemical society*, **1957**, *104*, 390-392.

[10] N. Alonso-Falleiros, Stephan Wolynec, *Materials Research*, **2002**, *5*, 77-84.

[11] M.N. EL-Haddad, *Carbohydrate Polymers*, **2014**, *112*, 595-602.

[12] K.F. Khaled, *Int. J. Electrochem. Sci.*, **2013**, *8*, 3974-3987.

[13] D. E. Tonini,J. M. Gaidis, *Corrosion of reinforcing steel in concrete*, Symposium on corrosion of metals, **1978**, 713.

[14] E.H. Yu, S. Cheng, B.E. Logan, K. Scott, *J Appl Electrochem*, **2009**, *39*, 705-711.

[15] T.F. O'Brien, T.V. Bommaraju, F. Hine, *Handbook of Chlor-Alkali Technology*, *Volume I: Fundamentals*.

[16] N. Souissi, E. Triki, *Materials and Corrosion*, **2010,** *61*, 695-701.

[17] L.L. Scribner, *The Measurement and Correction of Electrolyte Resistance in Electrochemical Tests*, **1990**, 1056.

[18] H.H. Hassan, K. Fahmy, *Int. J. Electrochem. Sci.*, **2008**, *3*, 29-43.

[19] H.H. Hassan, *Electrochimica Acta*, **2005**, *51*, 526-535.

[20] H.M. Ezuber, *Materials and Design*,**2014**, *59*, 339-343.

[21] M. Guzmán, R. Lara, *Int. J. Electrochem. Sci.*, **2014**, *9*, 3491-3500.

[22] L.Cáceres, T. Vargas, L. Herrera, *Corrosion Science*, 2007, *49*, 3168-3184.

[23]S. Neodo, D. Carugo, J.A. Wharton, K.R. Stokes, *Journal of Electroanalytical Chemistry*, **2013**, *695*, 38-46.

[24] R.S. Oguike,*Advances in Materials Physics and Chemistry*, **2014**, *4*, 153-163.

[25] Y.W. Jang, J.H. Hong, J.G. Kim, *Met. Mater. Int.*, **2009**, *15*, 623-629.

[26] S.A. Park, S.H. Lee, J.G. Kim, *Met. Mater. Int.*, **2012**, *18*, 975-987.